

Supplemental Material

Expanded Materials and Methods

Coronary artery tissues and human subjects

Freshly explanted hearts from orthotopic heart transplantation recipients were procured at Stanford University under IRB approved protocols and written informed consent. Participants were not compensated for this study. Hearts were arrested in cardioplegic solution and rapidly transported from the operating room to the adjacent lab on ice. The proximal 5-6 cm of three major coronary vessels (left anterior descending (LAD), left circumflex (LCX), and right coronary artery (RCA)) were dissected from the epicardium on ice, trimmed of surrounding adipose (and in some samples the adventitia), rinsed in cold phosphate buffered saline (PBS), and rapidly snap frozen in liquid nitrogen. Coronary artery samples were also obtained at Stanford University (from Donor Network West and California Transplant Donor Network) from non-diseased donor hearts rejected by surgeons for heart transplantation and procured for research studies. All hearts were procured after written informed consent from legal next-of-kin or authorized parties for the donors. Reasons for rejected hearts include size incompatibility, comorbidities, or risks for cardiotoxicity. Hearts were arrested in cardioplegic solution and transported on ice following the same protocol as hearts used for transplant. Explanted hearts were generally classified as ischemic or non-ischemic cardiomyopathy and prior ischemic events and evidence of atherosclerosis was obtained through retrospective review of electronic health records at Stanford Hospital and Clinics. The disease status of coronary segments from donor and explanted hearts was also evaluated by gross inspection at the time of harvest (for presence of lesions), as well as histological analysis of adjacent frozen tissues embedded in Tissue-Tek O.C.T. compound (Sakura) blocks. Frozen tissues were transferred to the University of Virginia through a material transfer agreement and Institutional Review Board approved protocols. All samples were then stored at -80°C until day-of-processing.

GWAS fine-mapping analyses

We used Summary-level Mendelian Randomization (SMR)³³ to prioritize candidate causal genes that underlie the vascular GWAS signals at the *UFL1-FHL5* locus. A summary of the GWAS datasets used for these analyses is provided in **Table S15**. SMR is a transcriptome wide association study (TWAS) method that tests whether the association of a variant with a

phenotype is mediated through changes in gene expression, while accounting for the linkage disequilibrium in the study population. We performed SMR using STARNET and GTEx artery tissue eGenes for all genes +/-500 kb of the FHL5 transcription start site (*FHL5*, *UFL1*, *GPR63*, *NDUFAF4*, *KLHL32*, *MMS22L*), using the 1000G European reference panel. We used the HEIDI (heterogeneity in dependent instruments) test to filter associations driven by linkage disequilibrium rather than pleiotropy ($p_{HEIDI} > 0.01$) as previously done³⁴. We considered $p_{SMR} < 0.008$ (0.05/6) and $p_{HEIDI} > 0.01$ as evidence of pleiotropy or causality.

In a complementary approach, we performed a Bayesian colocalization analysis using the R package, *coloc 4.0-3*^{31,32} to calculate the posterior probability that the GWAS and eQTL data share a common signal. We colocalized GWAS signals with GTEx and STARNET artery tissue eQTLs using the *coloc.signals* function with default priors ($p_1=1E-4$, $p_2=1E-4$, $p_{12}=1E-5$). We considered the $PP_4 > 0.80$ as evidence of colocalization.

We used the Bayesian fine-mapping tool, PAINTOR_V3³⁵ to prioritize CAD causal variants at the *UFL1-FHL5* locus. We included 1Mb around the lead CAD GWAS SNP, rs9486719 and computed Pairwise Pearson correlations for all bi-allelic SNPs based on the 1000G European reference panel. We incorporated human coronary artery ATAC-seq peaks from Turner et al⁴⁵ as functional annotations to calculate prior probabilities for the model. Following calculation of the posterior probability, we ranked SNPs based on this metric and identified the 95% credible set.

Human coronary artery smooth muscle cell immortalization and characterization

Primary human coronary artery SMCs (HCASMCs) were purchased from Cell Applications (Catalog #350-05a) and immortalized by lentiviral transduction of the hTERT-IRES-hygro construct (Addgene Plasmid #85140)⁵⁰ in 10 μ g/ml polybrene. Transduced cells were selected using 400 μ g/ml of hygromycin (Gibco) and maintained in SMC basal medium (SmBM) supplemented with SmGM-2 SingleQuots kit (PromoCell). The maintenance of similar levels of SMC marker gene expression (e.g., SM22- α) was confirmed via western blot. The transcriptomes of these immortalized SMCs (HCASMC-hTERT) were characterized via RNA-seq and correlated with RNA-seq data of the parental cell line⁹⁴. A principal component analysis was performed incorporating primary HCASMCs, HCASMC-hTERT, HEPG2, K562, and human umbilical vein endothelial cell (HUVEC) RNA-seq data (**Fig S7**). Fastq files for the

primary HCASMCs were extracted from Sequence Read Archive (SRA) (SRR7064063, SRR7058289, SRR7058290). Fastq files for HEPG2, K562, and HUVECs were downloaded from ENCODE.

Cell culture conditions

Primary HCASMCs and HCASMC-hTERT were maintained in SMC basal medium (SmBM) supplemented with SmGM-2 SingleQuots kit (PromoCell #C-22162), which includes 5% Fetal Bovine Serum (FBS), insulin, Fibroblast Growth Factor (FGF), and Epidermal Growth Factor (EGF). HEK293T (ATCC #CRL-3216) and A7r5 cells (ATCC #CRL-1444) were cultured in 10% FBS (Gibco) supplemented DMEM (Sigma-Aldrich) and maintained up to passage 10 (p10). All cell cultures were maintained at 37°C and 5% CO₂. HCASMC-hTERT was generated from passage 4 (p4) HCASMC (Cell Applications) and expanded up to passage 8 (p8). All experiments in this study were performed on HCASMC-hTERT between p8-p20.

Lentivirus generation and transduction

FHL5/FHL5-NLS cDNA was amplified from genomic DNA and cloned into the lentiviral vector, Lenti-III-EF1α (ABM #LV043) using EcoR1 and BamH1 restriction sites. The transfer vector, psPAX, (Addgene#12260), and pMD2.G (Addgene #12259) were transfected into HEK293T cells (ATCC #CRL-3216) cultured between p6-p10 in DMEM plus 10% FBS using Lipofectamine 3000 (Invitrogen) according to the manufacturer's protocol. The lentiviral containing supernatant was harvested at 24 and 48 hours post transfection and frozen at -80°C until use. A summary of the oligonucleotides and other reagents used is provided in **Table S16**.

HCASMCs/HCASMC-hTERT were transduced at 60% confluence with 500µl of lentiviral containing supernatant and 10 ng/ml polybrene (EMD-Millipore). The viral containing supernatant was removed the following day. After 48 hours, 1.0 µg/ml puromycin (Gibco) was added to the culture medium for antibiotic selection. Puromycin resistant cells were expanded, and overexpression was validated via qPCR and/or western blot.

CRISPR-dCas9-SAM/MPH activation of *FN1* and *FOXL1*

gRNAs targeting the *FOXL1* and *FN1* promoter (**Table S16**) were designed using CRISPick algorithm (<https://portals.broadinstitute.org/gppx/crispick/public>) and cloned into the

lentiSAMv2 (Addgene #75112) using the BsmBI restriction enzyme sites. HCASMC-hTERT were transduced with lentiMPHv2 (Addgene #89308) and lentiSAMv2 lentiviruses. Cell lines were selected with and maintained in SMC media with 400 ug/ml hygromycin and 5ug/ml blasticidin.

CRISPR-dCas9-p300 activation of *FHL5*

gRNAs targeting the cis-regulatory element (chr6:96577895-96579081) harboring the rs10872018 variant (**Table S16**) were designed using CRISPick algorithm (<https://portals.broadinstitute.org/gppx/crispick/public>) and cloned into the pLV-U6-gRNA vector (Addgene #83925) using the BsmBI restriction enzyme sites. HCASMC-hTERT were transduced with pLV-dCas9-p300 (Addgene #83889) and pLV-U6-gRNA lentiviruses. Cell lines were selected with and maintained in SMC media with 1.0 ug/ml puromycin and 5 ug/ml blasticidin.

Immunocytofluorescence and analysis

5,000 HCASMC-hTERT were plated onto glass coverslips and grown for 24 hours in complete media. Briefly, cells were washed with sterile PBS, fixed for 10 minutes with 4% formaldehyde and then washed 3 times for 5 minutes with PBS before permeabilization with 0.1%-TritonX for 15 minutes. The cells were blocked for 1 hour at room temperature with a solution containing 0.1%-Tween20 and 1% donkey serum in PBS, then incubated overnight with primary antibodies (1:500 FHL5, Novus NBP1-31660; 1:1000 Phalloidin-iFluor 594 conjugated, Abcam Ab176757) in a solution of 1% BSA in PBS. The next day, cells were washed with 0.1%-Tween-PBS prior to be incubated with secondary antibodies (1:1000 anti-rabbit IgG-Alexa488, Abcam Ab150073) for 2 hours at room temperature, washed 5 minutes 3 times with PBS, 0.1 mg/ml of DAPI was then added on the cells for 5 minutes. Cells were washed again 3 times for 5 minutes before being mounted on microslides using Aqua-Poly/Mount medium (Polysciences, #18606). Images were acquired using an Olympus epifluorescent microscope (BX41). Images were acquired using a camera Nikon DS-Fi3 (Version 110.04.3707.E9) with the imaging software NIS Element from Nikon (version 4.600), and then individual channels were merged using Image J (version 1.53). 126 images were taken from 3 replicates for each cell type.

To analyze FHL5 subcellular localization in FHL5 or FHL5-NLS expressing HCASMC, the ratio of nuclear/total FHL5 signal was calculated for each individual channel image. Briefly, images were converted from RGB into a binary black/white format. After applying a threshold to remove staining artifacts, the DAPI images were used to define a mask for the nuclei, which was then used in a bitwise operation to calculate the FHL5 nuclear specific signal from the corresponding channel. FHL5 signal quantification was performed by measuring the sum of weighted intensities (e.g., the dot product of 256 intensity levels and the count of the pixels in each intensity level) from the individual FHL5 image histograms. The ratio was then calculated by dividing the sum of weighted intensities of the FHL5 signal in the defined nuclear region by the FHL5 signal in the whole cell. A minimum of 225 cells were examined.

Immunofluorescence

Coronary arteries were embedded in OCT and cryosectioned at 8 μ m. Frozen slides were washed with sterile PBS twice for 2 minutes followed by fixation with formaldehyde at 4% for 10 minutes. Then slides were washed with PBS twice for 2 minutes and tissue were permeabilized with Triton X at 0.05% for 10 minutes. Coronary artery tissues were blocked with donkey serum at 10% for 1 hour followed by incubation overnight at 4°C with anti-rabbit-FHL5 (Novus, NBP-32600) at 1:100 dilution, anti-mouse- α -SMA (Santa Cruz Biotechnology, SC-53142) at 1:100 dilution, and anti-mouse-RUNX2 (SC-390351, Santa Cruz Biotechnology) at 1:300 dilution. Slides were washed with PBS-tween at 0.1% 3 times for 3 minutes each followed by incubation with secondary antibody (1:400) and F-Actin (ActinGreen™ 488 ReadyProbes, ThermoFisher Scientific, USA) for 1 hour at room temperature. Then slides were washed with PBS-t (PBS, 0.05% Tween 20), 4 times for 3 minutes each and slides were mounted with diamond mounting medium containing DAPI. Slides were visualized with the Leica TCS SP8 confocal microscopy station and micrographs were digitized with the Leica Application Suite X software. Representative images were chosen following three criteria: 1) most illustrative of the disease/healthy state, 2) most illustrative tissue integrity, and 3) most illustrative signal/noise in the section.

Luciferase reporter assay

The enhancer sequence (180bp) harboring the rs10872018-G or rs10872018-A was cloned into the pLUC-MCS (Agilent) vector. 400 ng of the luciferase reporter constructs (pLuc-MCS, pLuc-MCS-rs10872018-G, pLuc-MCS-rs10872018-A), 100 ng of each expression plasmid (pCGN-

SRF, pCDNA6-MYOCD, or pCMV6-empty), and 5ng of Renilla-luciferase were transfected into A7r5 cells using Lipofectamine 3000. (Invitrogen). The media was replaced 6 hours post transfection. Samples were prepared using the Dual Luciferase Assay Kit (Promega) according to the manufacturer's protocol 24 hours post transfection. The luciferase activity was measured using the SpectraMax L luminometer (Molecular Devices). The Firefly luciferase signal was normalized to the Renilla luciferase signal for each sample.

The FHL5 bound enhancer sequence was amplified from HCASMC-hTERT genomic DNA and cloned into the lentiviral luciferase reporter plasmid, pLS-MP-Luc (Addgene #106253). HCASMC-hTERT were transduced with 500 μ l of lentiviral-containing supernatant and the media was replaced the next day. Samples were prepared using the Dual-Glo Luciferase Assay system (Promega) 48 hours post transduction and the Firefly luciferase signal was normalized to total protein concentration determined using a Bradford colorimetric assay (Thermo Scientific 23225).

CRE luciferase reporter assay

HEK293T cells were transfected with 490 ng of pCRE-luc (Agilent #219075) and 10 ng Renilla-TK plasmid (Addgene #E2241) using Lipofectamine 3000 according to manufacturer's instructions. 24 hours post transfection, Firefly and Renilla luciferase intensity was quantified using the Dual-Glo Luciferase Assay kit (Promega). The resulting Firefly luciferase signal was normalized to the matched Renilla luciferase signal for each sample.

Collagen gel contraction assay

250,000 HCASMCs were embedded in a 2 mg/ml collagen solution (Advanced BioMatrix #5074). Following incubation at 37°C for 90 minutes, the solidified gels were detached, and 1 ml of media was added on top of each collagen lattice. After 18-24 hours at 37°C, the diameter of the collagen gels was measured and quantified using ImageJ.

SMC calcification and alizarin red staining

30,000 HCASMC-hTERT were maintained in DMEM (Sigma #D6429) supplemented with 10% FBS (Gibco #26140079), 10 mM β -glycerophosphate disodium salt hydrate (Sigma #G9422), 50 μ g/mL ascorbic acid (Sigma, #A8960), and 10nM dexamethasone (Sigma, #D2915) for 21 days, with media replaced every other day. Following 14 and 21 days of treatment, RNA was

extracted from cells for qPCR. Following 21 days of treatment, cells were washed 2x with 500 μ L of PBS and fixed with 4% paraformaldehyde (Thermo Scientific #28908) at room temperature for 15 minutes. Wells were rinsed twice with water and incubated with 500 μ L of alizarin red staining solution (Sigma, #TMS-008-C) for 20 minutes at room temperature. Excess dye was removed by rinsing with water. Alizarin red staining was quantitated by extraction of stained calcified material at low pH. 400 μ L of 10% acetic acid (Ricca Chemical #R0135000) was added to each well and incubated at room temperature for 30 minutes. The monolayer and acetic acid slurry was vortexed, heated to 85°C for 10 minutes, cooled on ice for 5 minutes, and centrifuged at 4°C at 20,000xg for 15 minutes. The supernatant was neutralized with 150 μ L of 10% ammonium hydroxide (Alfa Aesar 35575-AP) and OD405 was measured. Alizarin red concentration was determined relative to known concentrations of Alizarin Red standards.

SMC calcium quantification

SMCs were incubated with Fluo-4 AM (2.5 μ M; ThermoFisher #F14201) and pluronic acid (0.004%) at 37°C for 20 minutes⁹⁵. Images were then acquired at 30 frames per second using an Andor Revolution WD (with Borealis) spinning-disk confocal imaging system (Andor Technology) comprising an upright Nikon microscope with a 40X water-dipping objective (numerical aperture, 0.8) and an electron-multiplying CCD camera. Fluo-4 was excited using a 488 nm solid-state laser, and emitted fluorescence was captured using a 525/36 nm band-pass filter. Following baseline measurements, SMCs were treated with phenylephrine (5 μ M; Sigma). Ca^{2+} ionophore, ionomycin (10 μ M; Sigma #10634) was used at the end of the experiment to calculate the total maximum calcium concentration⁹⁶.

Images were analyzed using custom-designed SparkAn software^{97,98}. Fractional fluorescence traces (F/F_0) were obtained by region of interest (ROI) using polygon drawing on each cell, excluding the nucleus.

Estimates of $[Ca^{2+}]_i$ were made using the following equation,

$$[Ca^{2+}] = K_d \frac{F/F_{max} - 1/R_f}{1 - F/F_{max}}$$

where F is fluorescence measured within an ROI, Fmax is the fluorescence intensity of Fluo-4 at a saturating maximum Ca^{2+} concentration, K_d is the dissociation constant of Fluo-4 (340 nM)⁹⁹, and R_f (= 100) is the Fluo-4 AM maximum:minimum ratio measured at saturating and

zero Ca^{2+} concentrations¹⁰⁰. Fmax was obtained individually for each culture dish by adding the Ca^{2+} ionophore, ionomycin (10 μM), and 20 mM external Ca^{2+} at the end of the experiment. Fractional fluorescence (F/F_0) was determined by dividing the fluorescence intensity (F) within an ROI by the mean fluorescence value (F_0), determined from images collected before stimulation.

Alamar blue cell proliferation assay

HCASMC-hTERT (2,000 cells) were seeded into each well of 96-well plate in 100 μl SMC media. After 4 days, 10 μl of Alamar blue reagent (Thermo Fisher) was added to each well and incubated for 1 hour at 37°C. Fluorescence intensity was measured using the excitation wavelength of 540 nm and emission wavelength of 585 nm on a microplate reader.

Western blot analysis

Cells were lysed in 1X RIPA buffer (Millipore Sigma #20-188) supplemented with a protease inhibitor cocktail (Roche #11697498001). Protein concentration was determined by a BCA Protein Assay (Thermo Scientific #PI23225). 20 μg of protein lysate per sample was fractionated through 4-20% Tris-Glycine gel (Invitrogen #XP04205BOX) under denaturing conditions. Gels were transferred at 20V for 1 hour to 0.2 μm pore size PVDF membrane (Invitrogen #LC2002) using the Invitrogen Mini Gel Tank (Invitrogen #A25977). The PVDF membrane was blocked for 1 hour at RT in 5% non-fat dry milk (Lab Scientific #M0841) in PBS with 0.1% tween-20 (PBS-T) and incubated overnight at 4°C with primary antibody diluted in 5% non-fat dry milk. The following primary antibodies were used in western blots: anti-FHL5 (Abnova #H00009457-M01) at 1:1000 dilution, anti-HA (Abcam #ab9110) at 1:5000 dilution, anti-H3 (Cell Signaling #9715S) at 1:5000 dilution, anti-alpha smooth muscle Actin (Abcam #ab5694) at 1:2500 dilution, and anti-SM22 (Abcam #ab14106). The following day the membrane was washed 3x with PBS-T, incubated with a HRP conjugated secondary antibody (Abcam #ab205718) for 1 hour diluted 1:10000 in 5% non-fat dry milk. The signal was detected using chemiluminescent substrate (Thermo Scientific #34580) and visualized in a linear range on the Amersham Imager 600 (GE Healthcare). For FHL5 and CREB co-immunoprecipitation, HEK293T cells were co-transfected with recombinant human CREB1 and FHL5-HA/FHL5-NLS-HA expression plasmids. Immunoprecipitation was performed using anti-FHL5 followed by western blot analysis using anti-CREB or anti-HA antibodies.

Detection of p-MLC and MYLK

HCASMC-hTERT were serum starved for 48 hours and then stimulated with 10 μ M phenylephrine for 2 minutes. Cells were then washed with PBS and placed on dry ice. Proteins were precipitated using the trichloroacetic acid (TCA): acetone method. Briefly, cells were washed with cold 10% TCA and cold acetone two times. Cells were rinsed with 1x PBS, scraped off the plate into a 150 μ l Laemmli buffer and titrated through a 21-gauge syringe. 30 μ l of lysate were loaded onto an 4-12% polyacrylamide gel submitted to SDS-page electrophoresis. Proteins were then transferred onto a PVDF membrane, which was blocked and incubated overnight with the primary antibodies: pMLC (1:1000, Cell Signaling #3671), MLCK (1:2000, Abcam #ab76092). The second day, the membrane was incubated with appropriate HRP-conjugated secondary antibodies followed by chemiluminescent based detection (Thermo Scientific #34580) and signal acquisition on the Amersham Imager 600 (GE Healthcare).

Quantitative PCR analysis

RNA was extracted using the Quick-RNA Minoprep kit (Zymo Research # R1055). Equal amounts of RNA, quantified by the Qubit Fluorometer (Invitrogen #Q33326), was reverse-transcribed into cDNA the high-capacity RNA-to-cDNA kit (Applied Biosystems #4387406) according to the manufacturer's instructions. Taqman qPCR was performed in duplicate for each sample using the QuantStudio 5 qPCR instrument (ThermoFisher), normalized to GAPDH expression levels and analyzed via the standard $2^{-\Delta\Delta C_t}$ method. Alternatively, SYBR qPCR was performed in duplicate for each sample, normalized to U6 or GAPDH expression levels, and analyzed using the standard $2^{-\Delta\Delta C_t}$ method. All SYBR primers were pre-validated for single amplicons using high-resolution melt curve analyses in QuantStudio. qPCR primers are included in **Table S16**.

RNA-seq library preparation, sequencing, and analysis

HCASMC-hTERT

RNA was extracted from HCASMC-hTERT cells (HA, FHL5 or FHL5-NLS) using the Quick-RNA Miniprep kit (Zymo Research #R1054). The quality of RNA was assessed on the Agilent 4200 TapeStation. High quality samples, (RIN score > 8) were sequenced at the University of Virginia Genome Analysis and Technology Core in triplicate. Salmon¹⁰¹ was used to quantify transcripts

from demultiplexed fastq files. Data normalization and differential expression (DE) analysis was performed using DESeq2 (v1.30.1). The Wald Test as implemented in the standard DESeq2 pipeline was used to determine differentially expressed genes. Genes with FDR < 0.05 and log₂ fold change > 0.6 were considered significant. Gene ontology enrichment and pathway analyses were performed using the EnrichR web-server^{102,103} or ClusterProfiler (v4.1.4)^{104,105}.

Coronary artery tissues

RNA was extracted from ~50mg of frozen human coronary artery tissue using the Qiagen miRNeasy Mini RNA extraction kit (Qiagen #217004). Prior to column-based RNA isolation, the tissue was pulverized using a mortar and pestle and then homogenized in Qiazol lysis buffer using stainless steel beads in a Bullet Blender (Next Advances). RNA concentration was determined using Qubit 3.0 and RNA quality was determined using the Agilent 4200 TapeStation. Libraries were prepared from high quality RNA samples (RNA Integrity Number (RIN) > 5.5 and Illumina DV₂₀₀ > 75) using the Illumina TruSeq Stranded Total RNA Gold kit (catalog #20020599) and barcoded with TruSeq RNA unique dual indexes (catalog # 20022371). 150bp paired end sequencing was performed at Novogene on an Illumina NovaSeq S4 Flowcell to a medial depth of 100 million total reads per library. The raw passed filter sequencing reads obtained from Novogene were demultiplexed using the bcl2fastq script. The quality of the reads was assessed using FASTQC and the adapter sequences were trimmed using trimalore. Trimmed reads were aligned to the hg38 human reference genome using STAR v2.7.3a according to the GATK Best Practices for RNA-seq. To increase mapping efficiency and sensitivity, novel splice junctions discovered in a first alignment pass with high stringency, were used as annotation in a second pass to permit lower stringency alignment and therefore increase sensitivity. PCR duplicates were marked using Picard and WASP was used to filter reads prone to mapping bias. Total read counts and RPKM were calculated with RNA-SeQC v1.1.8 using default parameters and additional flags “-n 1000 -noDoC -strictMode” and GENCODE v30 reference annotation. The transcript and isoform expression levels were estimated using the RSEM package¹⁰⁶.

CUT&RUN assay, library preparation and sequencing

CUT&RUN assay was performed as previously described with few modifications¹⁰⁷. The detailed protocol can be found at <https://www.protocols.io/view/cut-amp-run-targeted-in-situ-genome-wide-profiling-14egnr4ql5dy/v3>. Briefly, 250,000 HCASMC-hTERT were washed

twice with wash buffer 20mM HEPES pH 7.5, 150mM NaCl, 0.5mM spermidine, 1x protease inhibitor). 10µl conA beads (Bang Laboratories #BP531) were washed three times with Binding Buffer and incubated on ice until use. Cells were incubated at RT for 10 minutes on an orbital shaker (nutator, VWR) with the activated conA beads. The mixture was incubated overnight at 4°C with primary antibody (rabbit anti-FHL5 or anti-HA or IgG) diluted in Antibody Buffer (1x Wash Buffer, 0.05% Digitonin, 2.5mM EDTA). All primary antibodies and secondary antibodies are described in Table S2. Next day, the unbound antibody was washed away with 1mL Dig-Wash Buffer (0.05% digitonin) twice. Samples were resuspended in 150µl Dig-Wash Buffer and incubated with diluted secondary antibody for 1 hour at RT. Unbound secondary antibody was washed away with three washes of Dig-Wash Buffer and then resuspended in 50µl Dig-Wash buffer. 2.5 µl of pAG-MNase (Epicyphe # 15-1016) was added to each sample and incubated for 1 hour at 4°C on a nutator. After washing away unbound pAG-MNase three times with Dig-Wash buffer and resuspension in 150 µl of Dig-Wash buffer, 1 mM CaCl₂ was added to activate MNase cleavage. Samples were incubated at 0°C for 30 minutes. 150 µl STOP Buffer (200 mM NaCl, 20 mM EDTA, 50 ug/mL RNASE A, 40 ug/mL glycogen) was added to halt digestion and the resulting DNA fragments was released into solution following Proteinase K digestion and purified via phenol-chloroform extraction. DNA pellets were dissolved in 30 µl of TE Buffer (1 mM Tris-HCl pH 8.0, 0.1 mM EDTA) and stored at 4°C overnight.

The CUT&RUN libraries were prepared as previously described^{53,54}. 10 µl of ERA buffer (4X T4 Ligase Buffer, 2 mM dNTP, 1 mM ATP, 10% PEG4000, 0.5U/µl T4 PNK, 0.05U/µl T4 DNA polymerase, 0.05U/µl of Taq DNA polymerase) was added to each sample. The samples were placed in a thermocycler with the following program: Cycle 1: 12°C /15 minutes, Cycle 2: 37°C/15 minutes, Cycle 3: 58°C/ 45 minutes, Cycle 4: 8°C Hold. 5 µl of 0.15 uM of annealed Illumina Truseq adapters and 40 µl of 2x Ligation Buffer (2x Rapid Ligase Buffer (Enzymatics #B101L) and 4 µl T4 Ligase (Enzymatics L6030-HC-L) were added. Samples were then incubated at 20°C for 25 minutes. Following adapter ligation, the libraries were amplified 14 cycles using NEBNext Q5 Ultra Master Mix (NEB #M0544L) and purified with 1.2X volume of Ampure Beads (Beckman CoulterCatalog #A63880). DNA was eluted into 20 µl of Tris-EDTA Buffer and stored at -20°C until sequencing. DNA concentration was determined using Qubit dsDNA High Sensitivity Assay (Invitrogen #Q32851) and library size was assessed using DNA High Sensitivity Tape-Station kit (Agilent #5067-5584). Libraries were pooled and paired-end

sequencing (2x42bp, 8bp index) was performed using the NextSeq 2000 instrument with the NextSeq 2000 P2 kit at the UVA Genomics Core.

CUT&RUN analysis

CUT&RUN libraries were analyzed using the CUT&RUN Tools pipeline^{55,108}. Briefly, adapter sequences were trimmed from demultiplexed reads using Trimmomatic¹⁰⁹ and filtered reads were aligned to the hg38 genome with bowtie2¹¹⁰. After removal of unmapped and duplicate reads using Picard¹¹¹, peaks were called using MACS2¹¹² with a threshold q value < 0.01 . The pooled IgG sample was used as the control in peak calling. The global settings in the pipeline were as described: <https://github.com/fl-yu/CUT-RUNTools-2.0>, aside from `organism_build=hg38`. The parameters for the individual software called by the pipeline were also left unchanged. Bigwig files for each sample were created using deeptools¹¹³ and visualized on the UCSC genome browser. Gene ontology analysis was performed through GREAT⁵⁹ using the basal-plus extension to define putative target genes of FHL5 peak set, with the whole genome used as background. Known motif enrichment in FHL5, CREB, and IgG binding sites was determined in HOMER (v4.11) using the `findMotifsGenome.pl` command. FHL5 peaks were annotated according to the nearest protein-coding gene in CHIPseeker⁵⁶. Differential expression analysis and FHL5 binding site data was integrated using the Binding and Expression Target Analysis (BETA) software package⁵⁸. BETA calculates a rank sum product score to reflect the likelihood of direct transcriptional regulation by incorporating both DEGs and epigenomic profiles. We used the following thresholds for expression changes: \log_2 Fold Change > 0.6 , and for binding: FDR < 0.05 and $Q < 0.01$ and signal value > 5 . We considered the BETA rank sum product $< 1E-3$ as evidence of direct transcriptional regulation.

GWAS SNP enrichment

We used the GREGOR software tool⁶² to determine the enrichment of GWAS risk variants in FHL5, CREB, and IgG binding sites. GWAS summary statistics were filtered to include SNPs $P < 5E-5$. This list of suggestive SNPs was pruned using PLINK (v1.9) to retain the most significant SNPs with pairwise LD (r^2) threshold < 0.2 in the 1000G European reference panel. We then used the default GREGOR parameters as described in <https://genome.sph.umich.edu/wiki/GREGOR>.

STARNET analyses

eQTL analysis

The STARNET cohort and datasets were described previously^{30,114}. The STARNET cohort includes 600 individuals with CAD and 250 control samples. RNA-seq libraries from cardiometabolic tissues (aorta, mammary artery, liver, subcutaneous fat, visceral fat, blood, and skeletal muscle) were prepared using the polyA and Ribo-Zero library preparation protocols. 50-100 bp single-end sequencing was performed using the Illumina HiSeq sequencer to a depth of 20-30million reads per sample. *Cis*-eQTLs and *trans*-eQTLs were identified using the Matrix QTL package.

Gene regulatory network analysis

Normalized gene expression for all STARNET tissues were used to construct co-expression modules using block-wise Weighted Gene Co-expression Network Analysis (WGCNA). The modules were annotated based on gene ontology enrichment analyses using the Fisher's exact test employed in the WGCNA package. Phenotypic correlations with clinical traits were calculated by aggregating Pearson correlation *P*-values for genes in the module by Fisher's method. Gene regulatory networks were inferred using the GENIE3 package with edges constrained by eQTL genes and transcription factor annotations. Key driver analyses were performed in the Mergenomics R package. The co-expression and gene regulatory network data can be accessed at <http://starnet.mssm.edu/>.

Coronary artery gene regulatory network analysis

WGCNA

Total RNA-seq data was filtered to exclude genes present in fewer than 20% of the samples. Hierarchical clustering was used to identify sample outliers (UVA047, UVA125). The remaining 15,720 genes and 148 samples were used as input into WGCNA⁴⁶ to detect gene modules. WGCNA calculates the co-expression of genes through an adjacency matrix based on co-expression similarity between the *i*-th gene and the *j*-th gene. Hierarchical clustering of these gene co-expression values was used to determine gene modules. Module detection was performed multiple times using iterativeWGCNA⁴⁷ to prune poorly fitting genes and generate more robust gene modules. Genes not assigned to any of the modules were designated to the gray module. Coexpression modules were visualized using Cytoscape.

Bayesian network construction

Bayesian networks for the *FHL5*-containing module were constructed using RIMBANET (Reconstructing Integrative Molecular Bayesian Networks)¹¹⁵. STARNET aortic tissue eQTL data were also used as genetic priors such that genes with *cis*-eQTLs are allowed to be parent nodes of genes with coincident trans eQTLs, but not vice versa. One thousand Bayesian networks were reconstructed using different starting random seeds. Edges that appeared in greater than 30% of the networks were used to define a consensus network.

Key driver analysis

Given a set of genes (G) and directed gene network (N), Key driver analysis (KDA) generates a subnetwork, N_G, defined as the set of nodes in N that are no more than h-layers from the nodes of G and subsequently computes the size of the h-layer neighborhood (HLN) for each node. The key driver score increases if the HLN was greater than $\mu + \sigma(\mu)$, where μ is average size of HLN. Total key driver scores for each node were computed by summing all scores at each h-layer scaled according to h, $\sum_{n=1}^h (1/n)$. Genes with key driver scores in the top 5% were annotated as module key drivers.

Data Availability

All raw and processed CUT&RUN and RNA-seq datasets are made available on the Gene Expression Omnibus (GEO) database (accession: GSE201572). The following publicly available datasets were used in this study: human coronary artery scATAC-seq generated by Turner et al. (accession: GSE175621), bulk human coronary ATAC-seq generated by Miller et al. (accession: GSE72696), bulk left ventricle and liver tissue ATAC-seq generated by the ENCODE project (<https://www.encodeproject.org/>). Bulk RNA-seq fastq files for human coronary artery SMCs (SRR705828, SRR705829, SRR706406) were downloaded from sequence read archive (SRA) using sratools. ENCODE bulk RNA-seq fastq files for HUVECs (ENCFF000DUK, ENCFF000DUH), HEPG2 (ENCFF982FAM, ENCFF564BSM) and K562 (ENCFF104ZSG, ENCFF695XOC) cells were downloaded from the ENCODE project (<https://www.encodeproject.org/>). Processed scRNA-seq data for human coronary arteries generated by Wirka et al. and carotid arteries generated by Alsaigh et al. are accessible at the PlaqView single-cell data portal (<https://www.plaqview.com>). Normalized gene expression levels and expression quantitative trait loci (eQTL) data are available at the Genotype-Tissue Expression (GTEx) portal website (<https://www.gtexportal.org>). Stockholm-Tartu Atherosclerosis Reverse Network Engineering Task (STARNET) eQTL data and GRNs are

available at <http://starnet.mssm.edu>. Summary statistics and gene annotations for cardiometabolic GWAS (hypertension, diastolic blood pressure, CAD, systolic blood pressure, BMI, and pulse pressure) were accessed through the Cardiovascular Disease Knowledge Portal (<https://cvd.hugeamp.org/>).

Code Availability

All custom scripts used are available at https://github.com/MillerLab-CPHG/FHL5_Manuscript. All software tools used in this study are publicly available and full names and versions are provided in the reporting summary.

Statistical analyses

Data in bar graphs are presented with mean \pm standard error of mean (SEM) with each point represented as an individual replicate. Data in box plots are presented with lines denoting the 25th, median and 75th percentile with each point representing an individual donor. Pairwise comparisons were made using the student's t test or Wilcoxon rank test as appropriate. Comparisons between more than two groups were assessed using a two-way ANOVA test or Kruskal-Wallis test for smaller sample sizes ($n < 6$). The normality of the data for larger sample sizes ($n > 6$) was assessed using the Shapiro-Wilk test, with $P > 0.05$, supporting a normal distribution. For each of these analyses, we considered $P < 0.05$ as significant. P-values < 0.01 are presented in scientific notation.

To identify differentially expressed genes, we used the false discovery rate (FDR) adjusted $P < 0.05$ threshold and $\log_2\text{FoldChange} > 0.6$. Heatmaps were created using the pheatmap package and represent normalized expression (Z-score) for genes, scaled across each row. Gene ontology enrichment analyses were performed relative to all expressed genes using Fisher's Exact Test, with a significant threshold of 5% FDR. A summary of the statistical tests, group comparisons and exact p-values are included in **Table S17**.

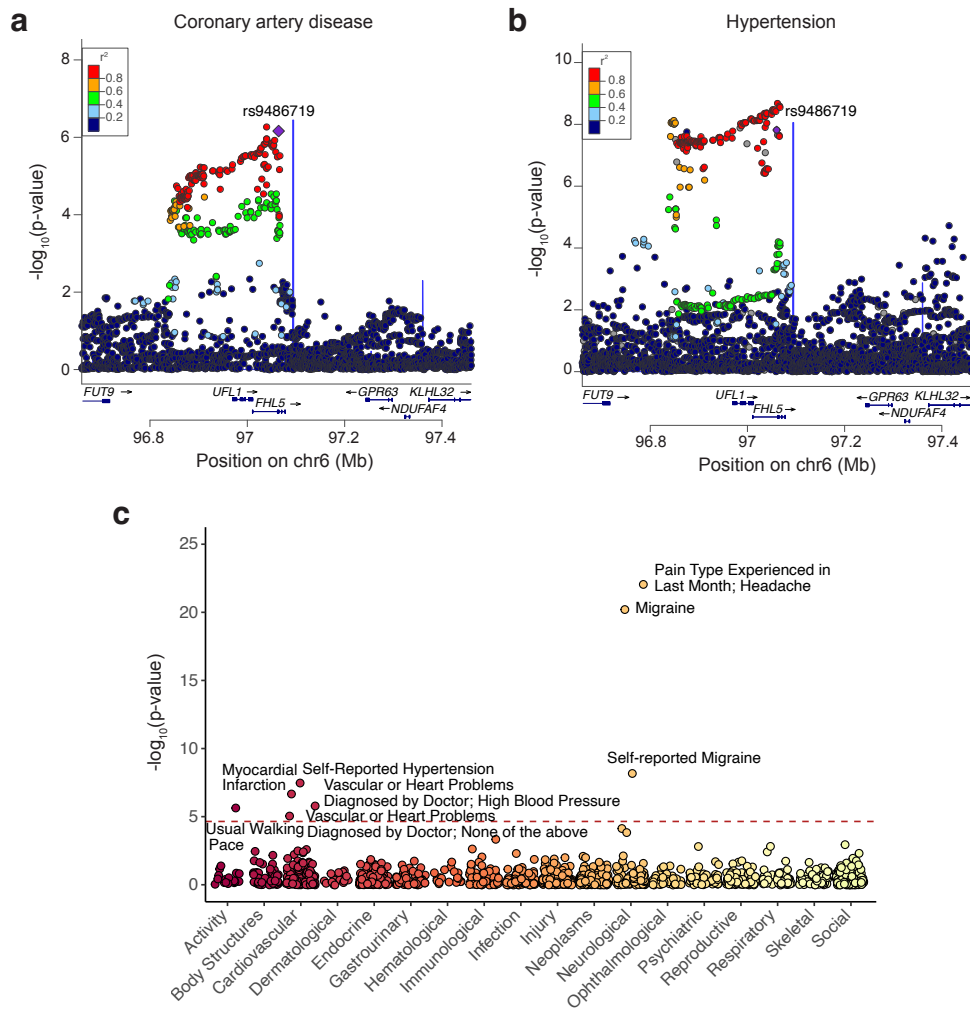


Fig. S1. *UFL1-FHL5* locus is associated with vascular diseases. LocusZoom plot highlighting the genetic association of the *UFL1-FHL5* locus with coronary artery disease (CAD) (a) as determined from the CARDIoGRAMplusC4D and UK Biobank meta-analysis, and hypertension (b) as determined from the UK Biobank. (c) Genetic association of rs9486719 across multiple phenotypes using GWAS studies reported in Phenoscanner, and traits organized in physiological categories on x-axis.

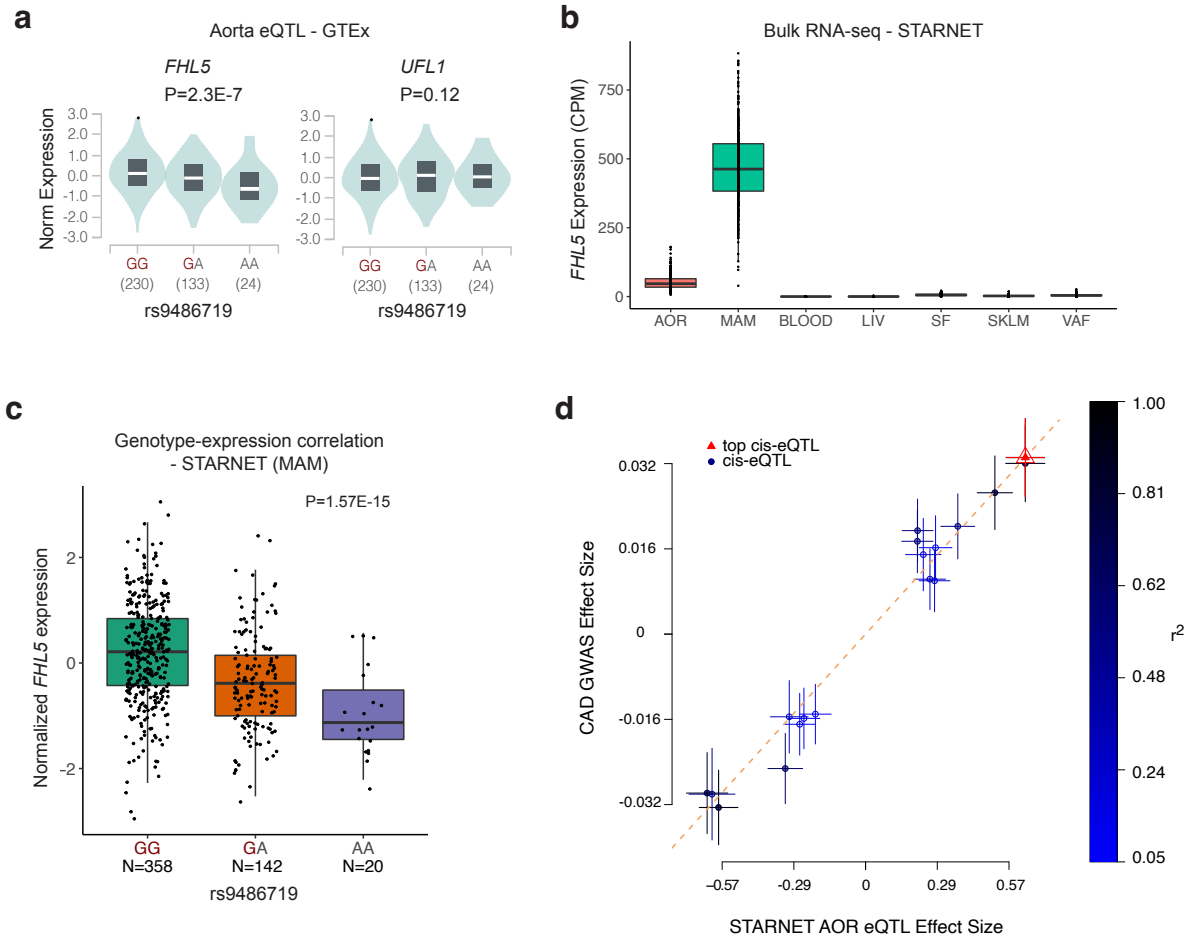


Fig. S2. *FHL5* is the top candidate causal gene at the CAD/MI *UFL1-FHL5* locus. (a) Violin plot showing rs9486719 allelic associations with *FHL5* gene expression (left) and *UFL1* (right) in GTEx (Aorta). (b) Normalized *FHL5* gene expression in counts per million (CPM) across STARNET cardiometabolic tissues: AOR: atherosclerotic aorta, MAM: mammary artery, LIV: liver, SF: subcutaneous fat, SKLM: skeletal muscle, VAF: visceral adipose fat. (c) Box plot showing rs9486719 association with *FHL5* expression in STARNET with the CAD/MI risk allele (rs9486719-G) highlighted in red. Box plots represent the median with the box spanning the first and third quartiles and whiskers as 1.5 times IQR. (d) Correlation of the effect size of MI risk alleles with *FHL5* eQTL effect size in STARNET AOR. Color scale depicts Pearson's r-squared values for the correlation of individual alleles.

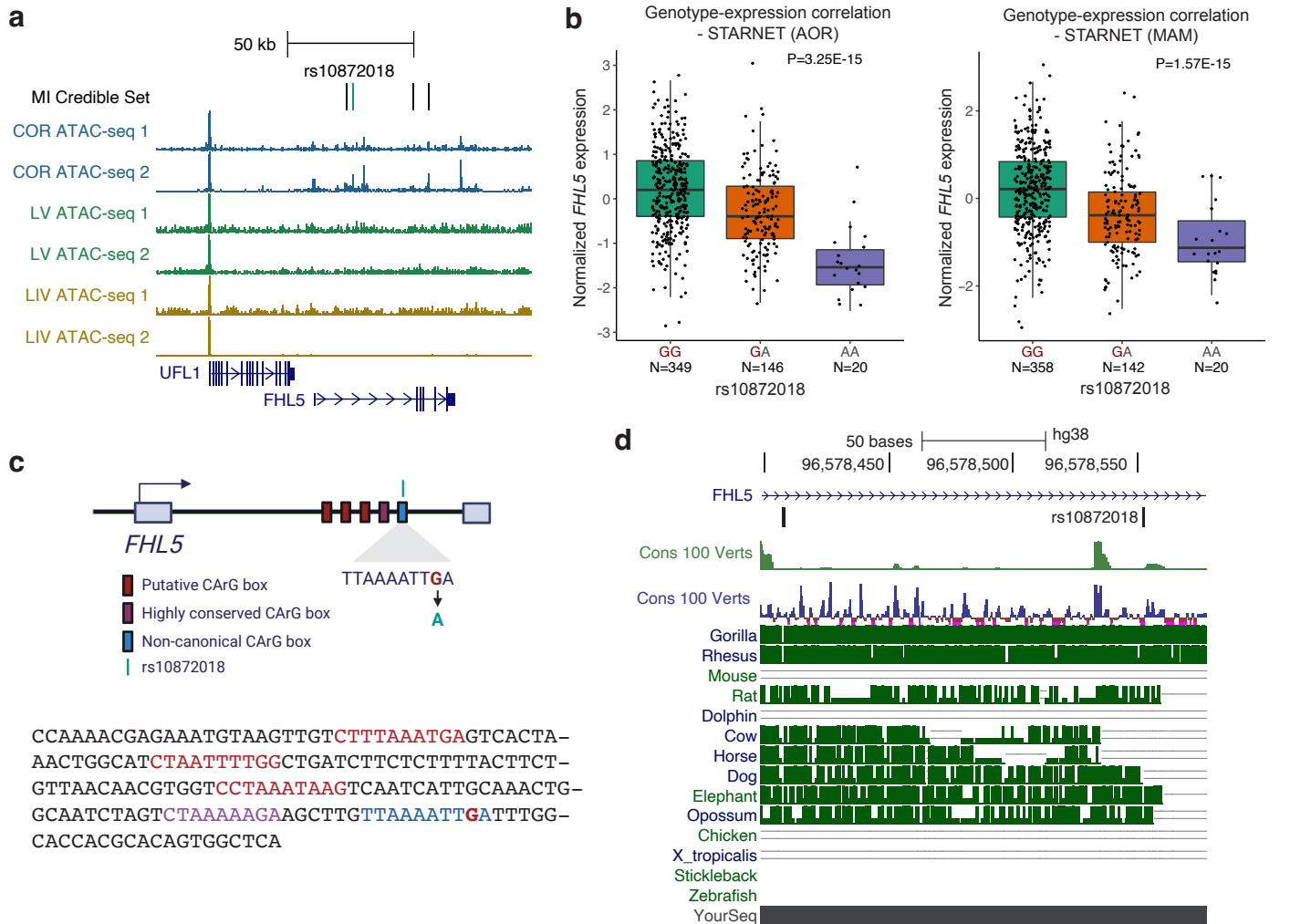


Fig. S3. rs10872018 is the top candidate causal variant underlying the MI *UFL1-FHL5* locus. (a) UCSC genome browser tracks for MI GWAS credible set of variants with ATAC-seq peaks in coronary artery (COR), left ventricle (LV), and liver (LIV), from two independent donors per tissue. Top candidate SNP rs10872018 highlighted in red. (b) Box plot showing rs10872018 association with *FHL5* expression in STARNET aorta (AOR) on left and mammary artery (MAM) on right, with the CAD/MI risk allele highlighted in red. Box plots represent the median with the box spanning the first and third quartiles and whiskers as 1.5 times IQR. (c) Schematic highlighting 5 putative CArG boxes in intron 1 of *FHL5*, including one highly conserved CArG box and the last motif (non-canonical CArG box) disrupted by rs10872018-A. Sequence of 180bp fragment used in reporter construct with putative CArG boxes highlighted in red or purple and non-canonical CArG box in blue containing rs10872018 (red). (d) UCSC genome browser screenshot highlighting sequence conservation of 180bp regulatory sequence containing rs10872018. 100 vertebrate conservation by PhastCons shown in green and basewise conservation by PhyloP shown in blue/red with selected species shown.

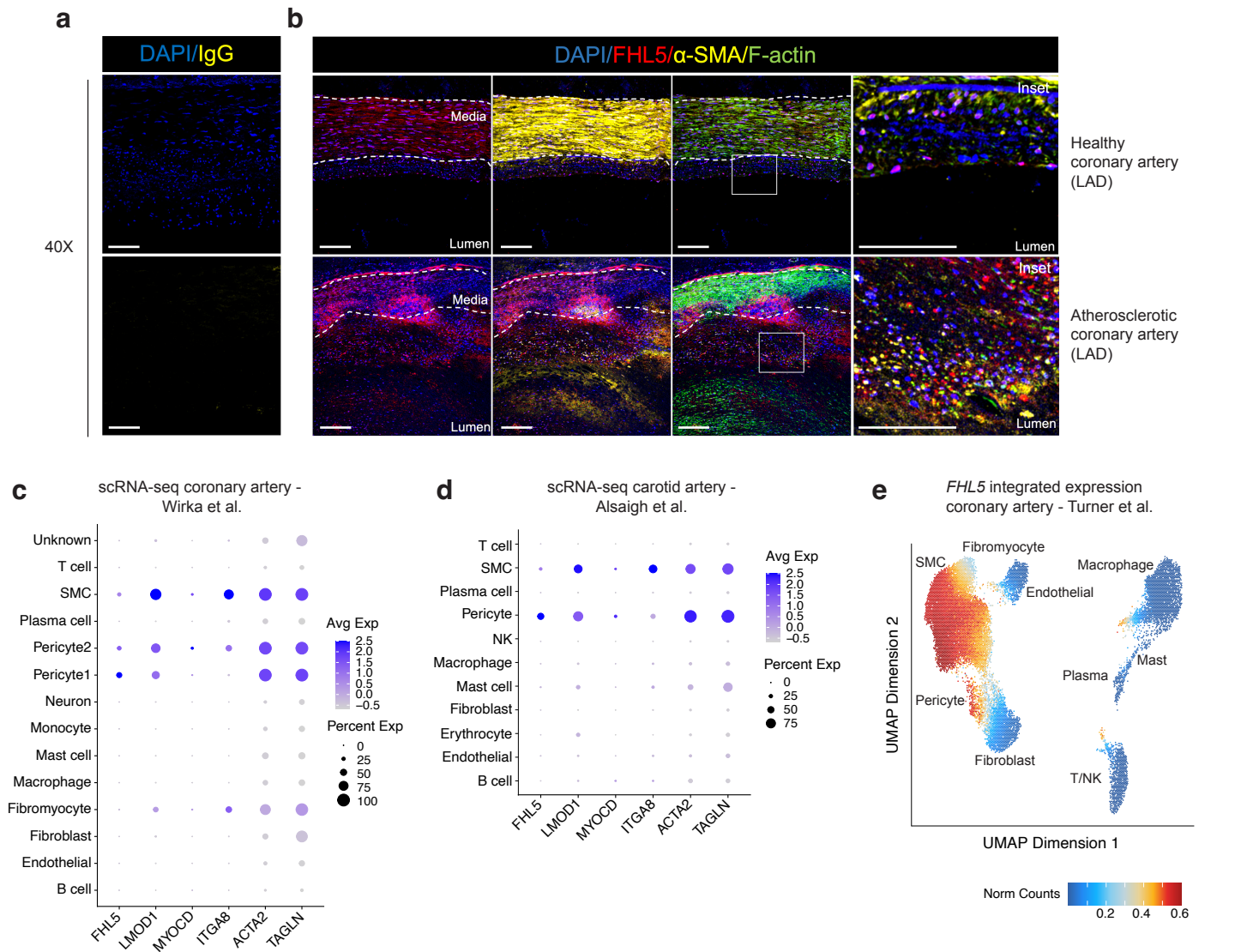
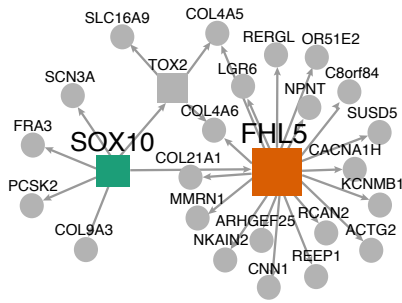
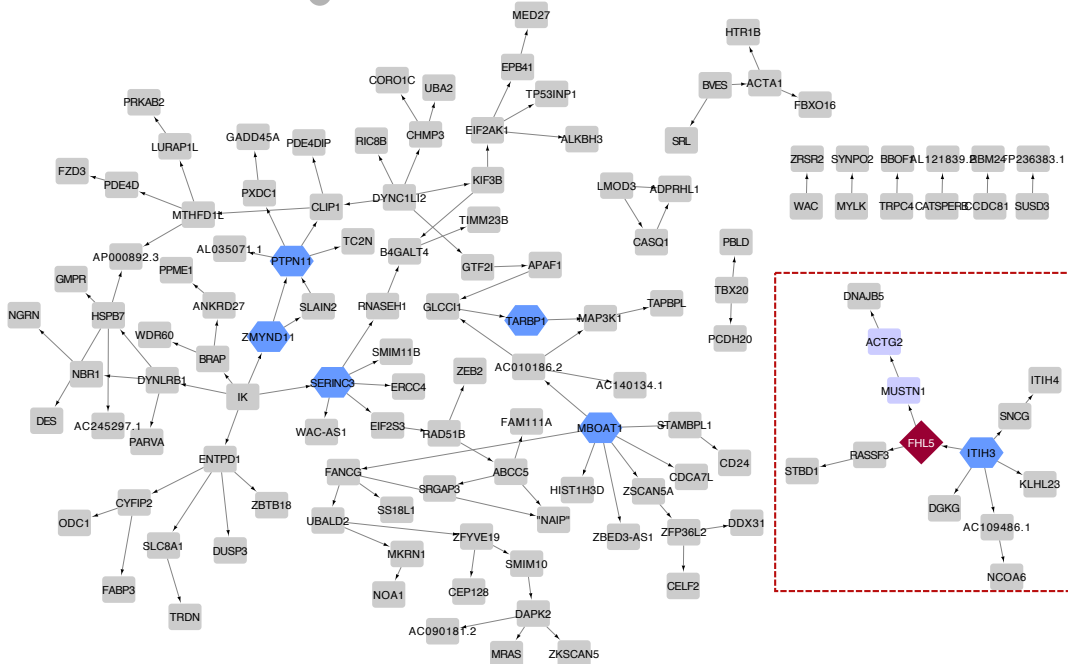


Fig. S4. *FHL5* gene expression is enriched in SMC and pericytes in human coronary arteries. (a) Coronary artery staining showing DAPI positive nuclei (top) and rabbit IgG negative control (bottom) with Alexa 647 secondary antibody. (b) Top panels, representative *FHL5* (red) co-staining with alpha-smooth muscle actin (α -SMA) (yellow) or F-actin (green), along with DAPI in healthy coronary artery tissue. Bottom panels, representative staining in atherosclerotic coronary artery. Images captured at 40X magnification. Inset panels show *FHL5* overlapping DAPI nuclei and α -SMA positive cells in the lesion. Results are representative of n=4 donors per group. Scale bars = 0.2 mm. (c) Dot plot showing average expression and percentage of cells expressing *FHL5* and other SMC markers in scRNAseq of subclinical atherosclerotic human coronary arteries (Wirka et al.). (d) Dot plot showing average expression and percentage of cells expressing *FHL5* and other markers in scRNAseq of healthy and atherosclerotic human carotid arteries (Alsaigh et al.). (e) UMAP plot showing *FHL5* integrated expression in SMC and pericytes using integrated coronary artery snATAC-seq and scRNA-seq dataset from Turner et al. Clusters are labeled by the main cell-type annotations after integration of the two datasets.

a *FHL5* as key driver gene in STARNET - Talukdar et al.



b



c

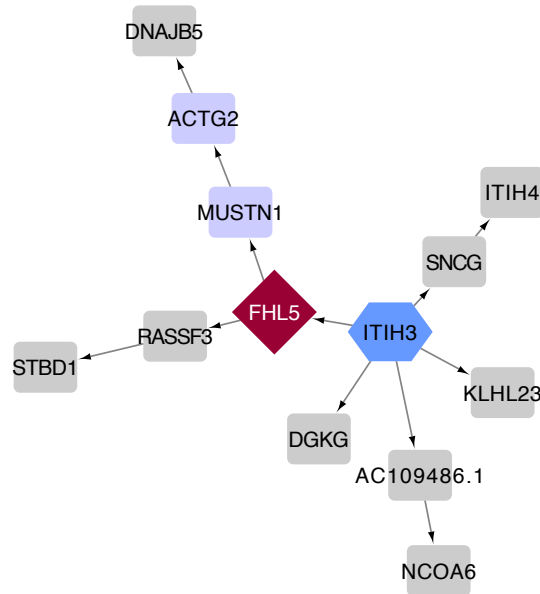


Fig. S5. *FHL5* gene regulatory network (GRN) in human coronary arteries. (a) Cross-tissue network analysis in STARNET identifies *FHL5* as a key driver gene (orange box) along with *SOX9* (green box) in a network enriched for CAD and ECM genes. Adapted from Talukdar et al. (b) Directed bayesian network showing *FHL5* GRN in human coronary arteries. Key drivers are highlighted in blue hexagons. Dotted red box denotes the *FHL5* subnetwork. (c) Zoomed in view of *FHL5* subnetwork. Key driver of subnetwork, *ITIH3*, depicted in blue hexagon. Downstream *FHL5* genes that function in SMC contraction biological process are highlighted in purple rectangles.

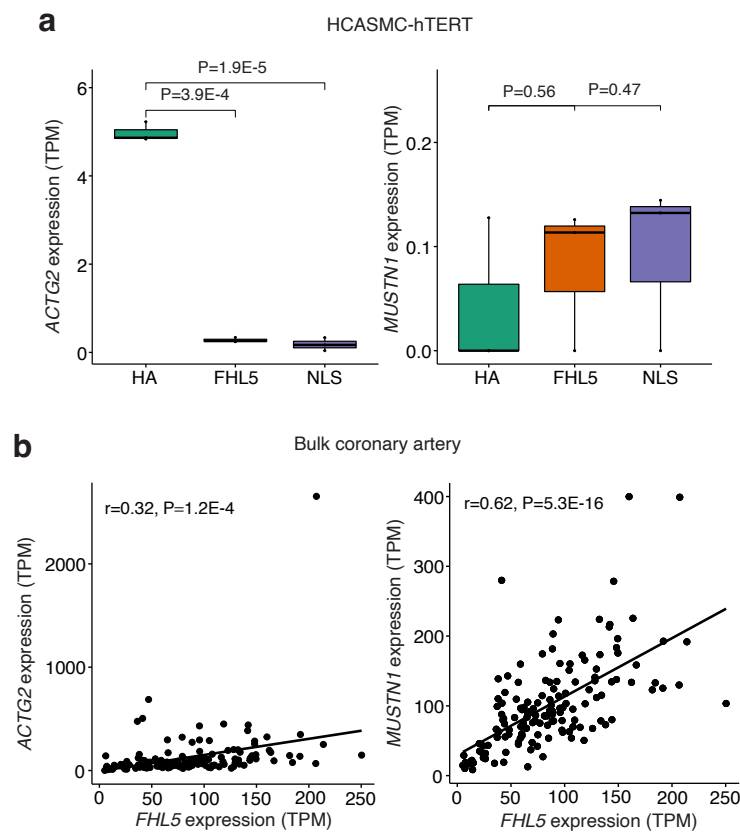


Fig. S6. Expression levels of FHL5 candidate downstream genes in SMC and coronary artery. (a) Normalized gene expression (TPM) of *ACTG2* (left) and *MUSTN1* (right) in HCASMC-hTERT overexpressing HA, FHL5, and FHL5-NLS. Box plots represent the median with the box spanning the first and third quartiles and whiskers as 1.5 times IQR. (b) Correlation between *FHL5* and *ACTG2* (left) and *MUSTN1* (right) gene expression (TPM) in bulk human coronary artery tissues (n=148). Each dot reflects a different patient sample. Pearson R correlation coefficient and p-values are shown.

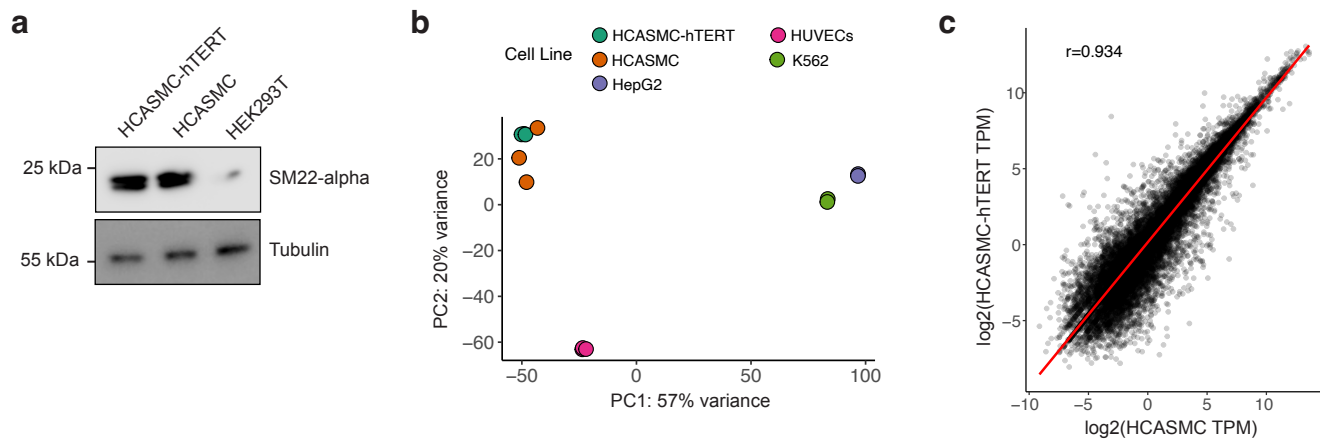


Fig. S7. Characterization of HCASMC-hTERT. (a) Western blot showing expression levels of SMC marker, SM22-alpha, in HCASMC-hTERT and the parental HCASMC (Cell Applications #2105). Tubulin is shown as a loading control. Molecular weights are shown for protein markers in PageRuler Plus ladder. (b) Principal component analysis (PCA) showing similarity in the transcriptomes of HCASMC-hTERT and primary HCASMC relative to HEPG2, HUVEC, and K562 cells. (c) Pearson correlation of HCASMC-hTERT and parental primary HCASMC transcriptomes shown as \log_2 normalized gene expression (transcripts per million (TPM)).

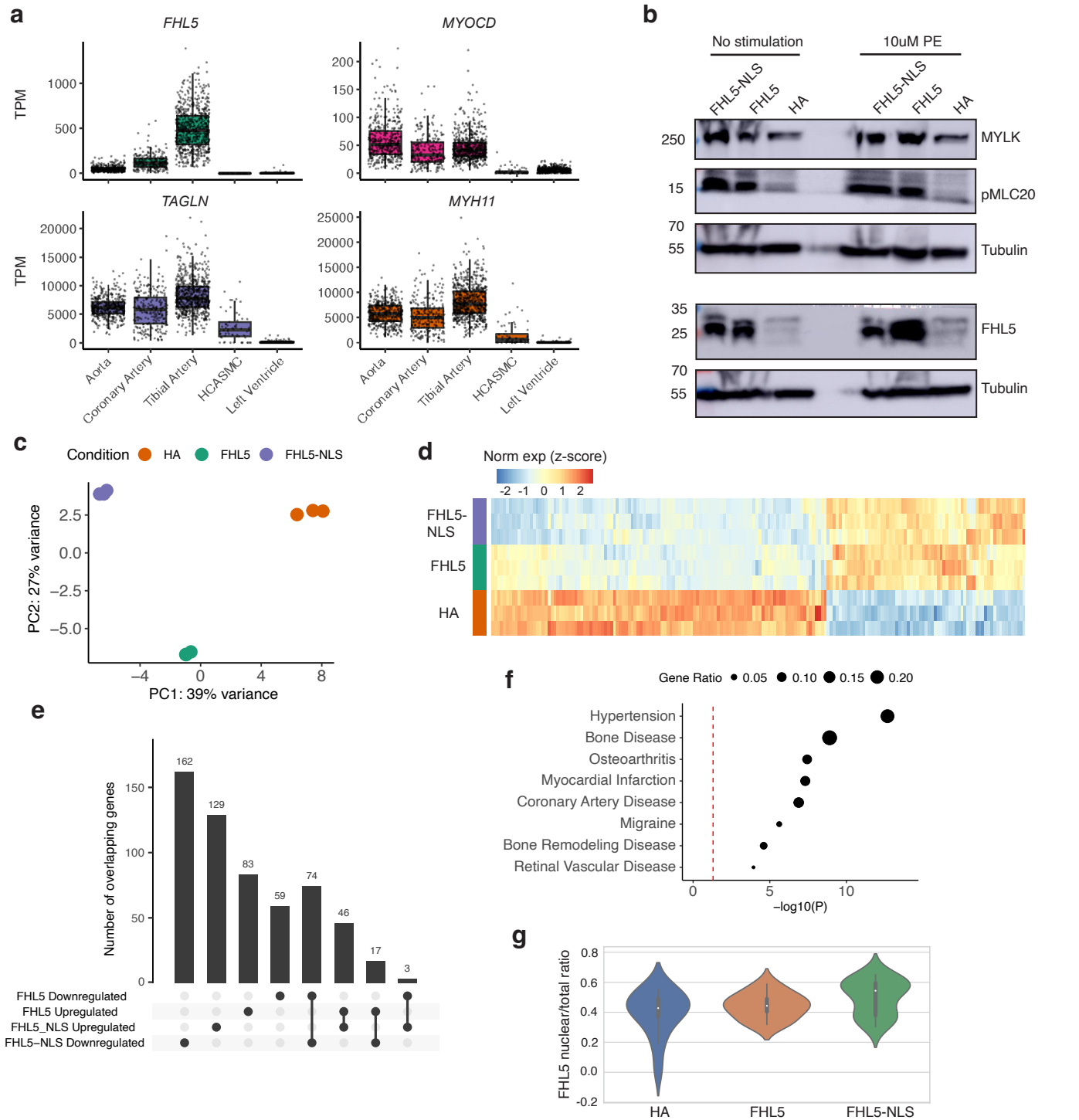


Fig. S8. Comparison of FHL5 and FHL5-NLS differentially expressed genes. (a) Normalized expression level in transcripts per million (TPM) of *FHL5* and SMC markers in GTEx human aorta (N=432), coronary artery (N=240), tibial artery (N=663), left ventricle (N=432) and HCASMC (N=61). (b) HCASMC-hTERT overexpressing FHL5-NLS, FHL5, and HA were stimulated with 10uM phenylephrine (PE). Western blot of samples under both basal (left) and PE stimulated conditions (right) was performed using the indicated antibodies. Molecular weight markers (kDa) are indicated by colored lines. (c) PCA of normalized HA, FHL5, and FHL5-NLS using RNAseq transcriptomes (n=3 per group). (d) Heatmap showing log₂ normalized expression of 168 DEGs derived from the union of FHL5 and FHL5-NLS significantly upregulated and downregulated DEGs and clustered using n=3 biological replicates per group. (e) Upset plot showing overlap between FHL5 and FHL5-NLS upregulated and downregulated genes. (f) Disease enrichment analysis of the FHL5 DEGs showing enrichment of disease ontology (DO) terms from 381 FHL5 DEGs against the whole transcriptome as a background. P-values shown are unadjusted. (g) Quantitated FHL5 immunofluorescence in HA, FHL5, and FHL5-NLS HCASMC-hTERT showing nuclear/total FHL5 protein ratio. Results are from >225 analyzed cells from triplicates for each cell type. Box plots represent the median spanning the first and third quartiles and whiskers as 1.5 times IQR.

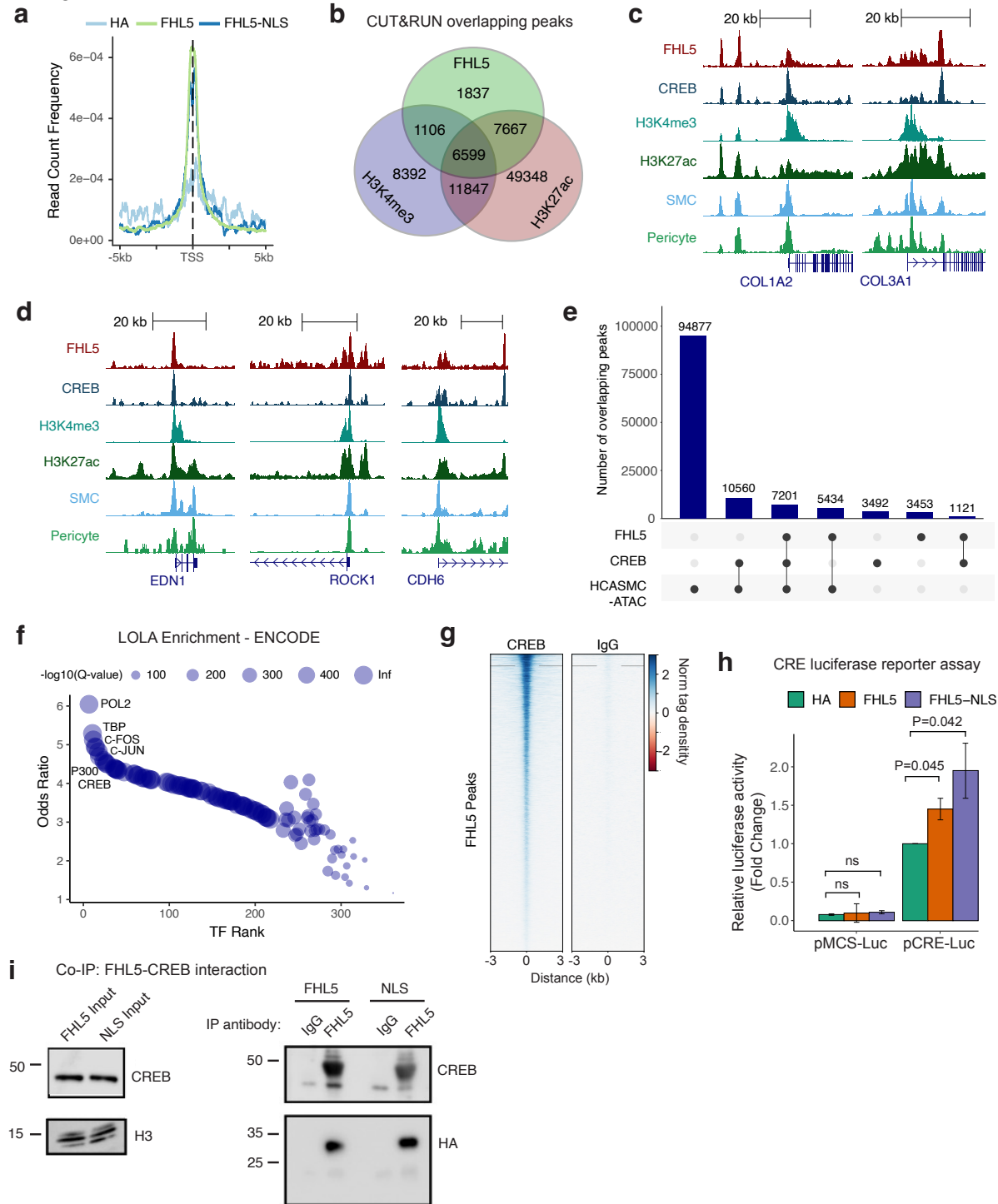


Fig. S9. FHL5 interacts with CREB to transcriptionally regulate extracellular matrix and cell adhesion genes. (a) Density plot of FHL5 (light green) and FHL5-NLS (dark blue) genome-wide CUT&RUN peaks centered on transcription start sites (TSS). (b) Overlap of FHL5, H3K27ac, and H3K4me3 CUT&RUN peaks in SMCs. (c-d) UCSC genome browser tracks for FHL5, CREB, H3K27ac and H3K4me3 CUT&RUN performed in HCASMC-hTert, as well as snATAC-seq for SMCs and pericytes from human coronary artery (Turner et al. 2022) near ECM genes *COL1A2* and *COL3A1* (c), and cell adhesion genes *EDN1*, *ROCK1*, and *CDH6* (d). (e) Overlap of FHL5 and CREB SMC binding sites with primary human coronary artery SMC ATAC-seq peaks. (f) LOLA enrichment of FHL5 binding sites in ENCODE transcription factor (TF) ChIP-seq datasets, highlighting AP-1 family TFs, CREB, as well as transcription machinery proteins RNA polymerase II (POL2) and TATA binding protein (TBP), and transcriptional activator P300. (g) Heatmap of CREB binding sites relative to the center of FHL5 binding sites, compared to non-specific IgG binding sites. (h) Relative fold change in CRE-luciferase reporter activity normalized to Renilla after 24 hours post transfection with pCRE-Luc and expression plasmids for HA, FHL5 or FHL5-NLS in HEK293T cells. Results are mean \pm SEM of triplicates from a representative experiment (n=2). (i) Co-immunoprecipitation in HEK293T cells co-transfected with CREB1 and FHL5-HA/FHL5-NLS-HA expression plasmids. IP performed using anti-FHL5 antibody followed by immunoblotting for CREB or HA.

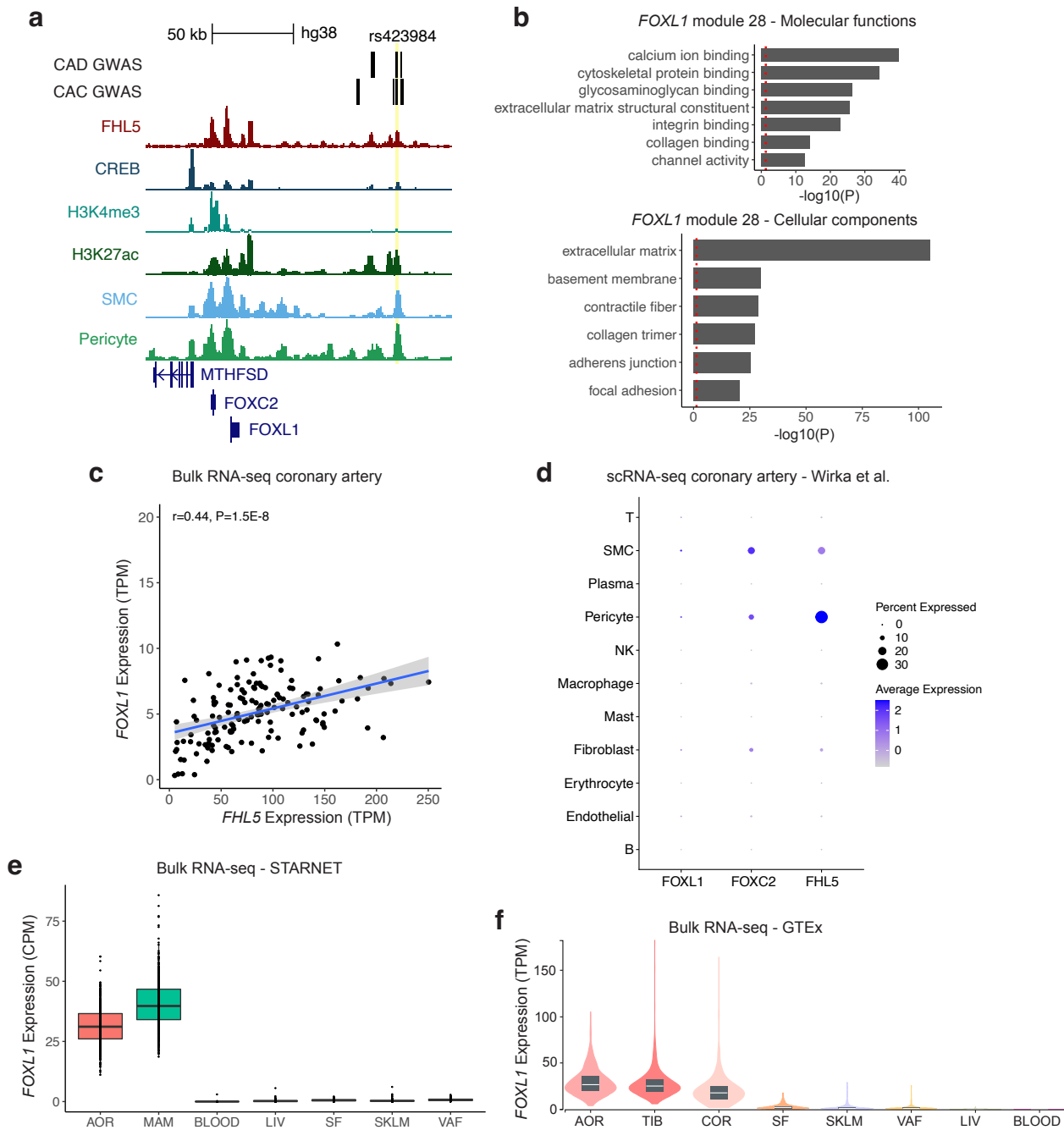


Fig. S10. FHL5 regulation of FOXL1 may contribute to the underlying mechanism of its association with CAD/MI.

(a) UCSC genome browser tracks of the *FOXC2-FOXL1* locus for the top credible SNP rs423984 (95% credible set for MI) highlighted in yellow, FHL5, CREB, H3K27ac and H3K4me3 CUT&RUN, and snATAC-seq for SMCs and pericytes from human coronary artery (Turner et al. 2022). (b, upper) Top molecular functions enriched in module 28. (b, lower) Top cell compartments enriched in module 28 genes. P-values shown were adjusted using Bonferonni test for multiple comparisons. The red dotted line corresponds to a nominal threshold of $FDR < 0.05$. (c) Pearson correlation of *FHL5* and *FOXL1* gene expression from bulk RNA-seq of human coronary arteries (N=148). (d) Dot plot showing enrichment of *FOXL1*, *FOXC2* and *FHL5* gene expression in SMC and pericytes in human coronary artery single-cell RNA-seq (Wirka et al.). (e) Normalized expression level in counts per million (CPM) of *FOXL1* in cardiometabolic tissues profiled in STARNET bulk RNA-seq analysis. (f) Normalized expression level in transcripts per million (TPM) of *FOXL1* in bulk RNA-seq of GTEx cardiometabolic tissues. AOR: aorta, MAM: mammary artery, BLOOD: whole blood, LIV: liver, SF: subcutaneous adipose fat, SKLM: skeletal muscle, VAF: visceral adipose fat, TIB: tibial artery, COR: coronary artery.